Development of a lead-free composite solder from Sn–Ag–Cu and Ag-coated carbon nanotubes

S. Chantaramanee · S. Wisutmethangoon ·
L. Sikong · T. Plookphol

Abstract The microelectronic applications of lead-free solders pose ever-increasing demands. We seek to improve the solder by forming composites with Ag-coated single-walled carbon nanotubes (Ag-coated SWCNTs). These were incorporated into 96.5Sn–3.0Ag–0.5Cu solder alloy with an ultrasonic mixing technique. Composite solder pastes with 0.01–0.10 wt% nanotube reinforcement were prepared. The wettability, melting temperature, microstructure and mechanical properties of the composite solders were determined, and their dependency on nanotube loading assessed. Loading with 0.01 wt% Ag-coated SWCNTs improved the composite solder's wetting properties, and the contact angle was reduced by 45.5 %, while over loading of the coated nanotubes up to 0.10 wt% degraded the wettability. DSC results showed only slight effects on the melting behavior of the composite solders. Cross-section microstructure analysis of the spreading specimens revealed uniform distribution of the intermetallic compounds throughout the solder matrix, and EDS analysis identified the phases as β-Sn, Ag_3Sn and Cu_6Sn_5. The mechanical properties of composite specimens, compared with those of unloaded 96.5Sn–3.0Ag–0.5Cu solder, had a maximal improvement in the shear strength of 11 % when the nanotube loading was 0.01 wt% of Ag-coated SWCNTs.

S. Chantaramanee · L. Sikong · T. Plookphol (✉)
Department of Mining and Materials Engineering, Faculty
of Engineering, Prince of Songkla University, Hat Yai,
Songkhla 90112, Thailand
e-mail: thawatchai.p@psu.ac.th

S. Wisutmethangoon
Department of Mechanical Engineering, Faculty of Engineering,
Prince of Songkla University, Hat Yai, Songkhla 90112,
Thailand

L. Sikong
Center of Excellence in Nanotechnology, Prince of Songkla
University, Hat Yai, Songkhla 90112, Thailand

1 Introduction

Tin–lead (Sn–Pb) solder alloy has been widely used in electronic packaging industry for decades because it has good mechanical, thermal and electrical properties [1]. However, lead (Pb) is considered a hazardous substance, and restrictions on using Pb in electronic and electrical devices were implemented [2]. A large number of lead-free solder alloys have since been developed, to replace the Pb-containing ones. Tin–silver–copper solders, for example 96.5Sn–3.0Ag–0.5Cu (SAC305), are currently widely used lead-free solder alloys [3]. The trend in electronics packaging is towards the solder joints getting smaller and smaller in size, and composite and nanocomposite solders have been developed to improve the thermo-mechanical and electrical properties of the ultra-fine solder joints [4–6]. Carbon nanotubes (CNTs) are interesting materials, first discovered by Iijima [7]. Their characteristics have been investigated and tuned by modifications, by many researchers, for practical applications. Nai et al. [8–13] have studied the effects of *multi*-walled carbon nanotubes on Sn–Ag–Cu composite solders: the mechanical and wetting properties improved, while the melting temperatures were not affected. Furthermore, shear tests conducted on lap-shear solder joints showed improved shear strength, in comparison to the monolithic Sn–Ag–Cu composite solders. A typical use of *single*-walled carbon nanotubes (SWCNTs) is in a one-dimensional conductor. It may find important uses in nano-electronic devices, so the electronic properties of SWCNTs are actively studied [14]. Another application of SWCNTs is as a potential reinforcement in composite materials [15–17], since their theoretical strength is equal to steel. However, the

interfacial adhesion between the SWCNTs and the metal matrix is still poor because the nanotubes' surfaces are not active and do not have catalytic effects [18]. Electroless plating of CNTs with catalytic metals has been demonstrated as an effective way to improve surface activity. Previous studies reported that some metals and alloys were deposited on the CNTs surface to improve its wettability, for example by coating CNTs with Ag [18], Ni [19–21], Cu [22, 23], Sn [24], Ni–N [25], Au [26], Ni–P [27] and Co [28]. In the past few years, Han et al. [29–31] incorporated the Ni-CNTs in Sn–Ag–Cu composite solders with improved mechanical properties, including creep indentation. However, the shear strength of composite solder joints decreased with thermal cycles after addition of Ni-CNTs in the composite solders. Zhao et al. [32] demonstrated that Ag-coated MWCNTs are wetted to a certain degree by melted Sn, and embedded well in the matrix. Furthermore, Ag element is naturally compatible with Sn–Ag–Cu solder [33]. Ag atoms can also form a continuous coating on the MWCNTs with a significant binding energy [18]. Thus, Ag was here chosen as the coating material, and the Ag-coated single-walled carbon nanotubes (Ag-coated SWCNTs) were synthesized and used as a reinforcement in the present study.

Accordingly, the present study investigates the effects of adding varying quantities of Ag-coated SWCNTs into 96.5Sn–3.0Ag–0.5Cu composite solders. The wettability, melting temperature, microstructural morphology, and solder joints with the addition of different loadings of coated nanotubes, were assessed. In particular, the effects of nanotube loading on the mechanical properties of the composite solders were investigated.

2 Experimental procedures

2.1 Materials

In this study, 96.5Sn–3.0Ag–0.5Cu solder powder with a particle size of 20–45 μm (Type 3) was used as the matrix alloy. The powder solder was obtained from Thailand Smelting and Refining Company Limited (THAISARCO), Phuket, Thailand. Its composition is shown in Table 1. The reinforcement used was SWCNTs, 0.5–3.0 μm long and 1–2 nm diameter, purchased from Chengdu Organic Chemical Company Limited, China. A SEM image of the nanotubes is available in Fig. 1a.

**Table 1** Chemical composition of SAC305 lead-free solder alloy (wt%)

Sn	Ag	Cu	Au	Pb	Sb	As	Bi	In	Fe
Bal.	2.80–3.20	0.30–0.70	0.05	0.05	0.05	0.02	0.02	0.01	0.01

Table 2 Melting temperatures of SAC305 + Ag-coated SWCNTs solder composites at different weight percentages of SWCNT additions

Material	SWCNTs (wt%)	Melting temperature (°C)	
		Onset temperature	Peak temperature
SAC305	–	218.70	221.50
SAC305-0.01 Ag-coated	0.01	218.59	220.16
SAC305-0.04 Ag-coated	0.04	218.00	220.67
SAC305-0.07 Ag-coated	0.07	219.15	222.00
SAC305-0.10 Ag-coated	0.10	218.44	220.83

2.2 Synthesis of Ag-coated single-walled carbon nanotubes (Ag-coated SWCNTs)

Single-walled carbon nanotubes were Ag-coated by an electroless plating method. The procedure can be divided into four steps: oxidation, sensitization, activation and plating [18]. First, the SWCNTs were oxidized and purified by refluxing in a 3:1 boiling mixture of concentrated HNO_3 and H_2SO_4 for 10 h. Then, the SWCNTs were washed and filtered three times with distilled water, and dried in air at room temperature. The oxidized SWCNTs were put in an aqueous solution (previously aged for 72 h at room temperature) of 0.1 M $SnCl_2$/0.1 M HCl, stirred at room temperature for 30 min, then filtered and rinsed with distilled water three times. Next, the sensitized SWCNTs were immersed in an aqueous mixture of 0.0014 M $PdCl_2$ and 0.25 M HCl at room temperature, stirred for 30 min, then filtrated and rinsed three times with distilled water. Lastly, the activated SWCNTs were put into an Ag-plating solution. The solution was made by mixing the solutions of $AgNO_3$ 10 kg/m^3, $NH_3 \cdot H_2O$ 1.5 vol% and HCHO (added later) 3.0 vol%. In the 30 min deposition process, the bath was at room temperature. After that, the Ag-coated SWCNTs were filtered, rinsed three times with distilled water, dried in air and stored in a vial to protect the surfaces from oxidation. During oxidation, sensitization, activation and electroless plating, the reaction mixture was ultrasonically dispersed with Model VC750, 20 kHz, 750 W (Sonics & Materials, Inc., USA) at 40 % amplitude. The nanotubes were filtered with an 0.2 μm pore nylon membrane filter under vacuum. The nanotube surfaces after electroless plating were observed with a scanning electron microscope (SEM) Model JSM-5800LV, JEOL, with an image shown in Fig. 1b.
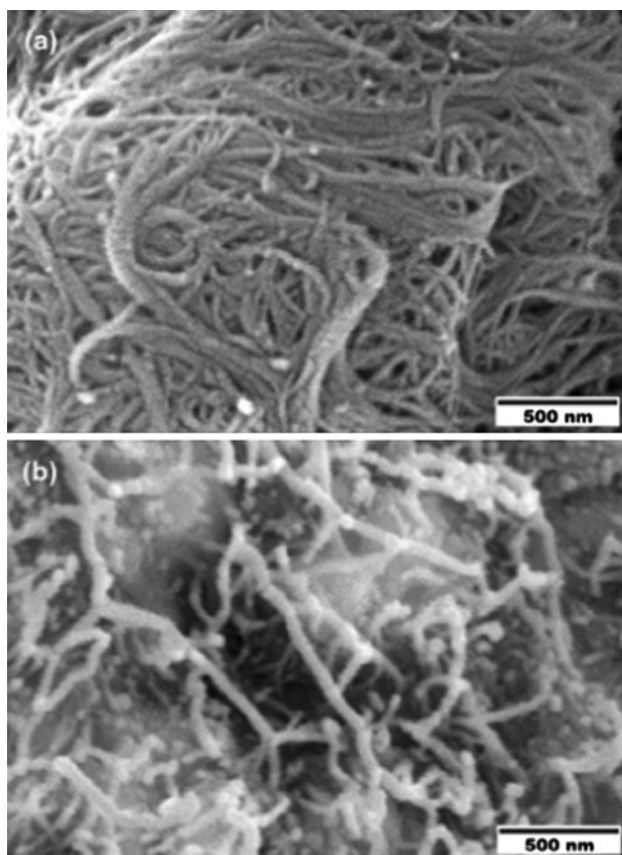
Fig. 1 SEM micrographs of **a** un-coated SWCNTs and **b** Ag-coated SWCNTs

2.3 Preparation of nanotube loaded composite solder pastes

The lead free 96.5Sn–3.0Ag–0.5Cu solder powder was loaded with either un-coated single-wall carbon nanotubes (un-coated SWCNTs) or Ag-coated single-wall carbon nanotubes (Ag-coated SWCNTs). Varying weight percentages of each type of nanotubes (0, 0.01, 0.04, 0.07 and 0.10) were incorporated into the solder matrix to synthesize two different systems of lead-free solder composites. The materials synthesized here are designated as SAC, SAC-0.01 un-coated, SAC-0.04 un-coated, SAC-0.07 un-coated, SAC-0.10 un-coated, SAC-0.01 Ag-coated, SAC-0.04 Ag-coated, SAC-0.07 Ag-coated and SAC-0.10 Ag-coated, in the forthcoming sections. The synthesis procedure was as follows. In the first step, the desired amount of solder powder, un-coated SWCNTs or Ag-coated SWCNTs were pre-weighted. Prior to blending, ethanol was added to the solder powder, then the nanotubes were added and ultrasonically mixed at 40 % amplitude, for 2 min; and dried at 80 °C. Similarly, a rosin mildly active (RMA-223) flux was added under sonication. The weight ratio of the composite solder powder and the flux was 9:1. Again, the sonication used 40 % amplitude for 2 min to ensure uniform distribution of the components. Lastly, the pastes were sealed immediately after being mixed, to avoid oxidation, and preserved in a refrigerator to delay dissolution of the paste.

### 2.4 Solder wettability test

Solder wettability was characterized by melt contact angle determination from solidified drops. The substrate wetted was a copper plate 25.4 mm × 25.4 mm × 0.2 mm with 99.99 % purity, and a surface roughness of Ra = 0.594 μm measured with Mitutoyo Surftest SJ-301. Before the experiment, the copper surface was cleaned with ethanol for 5 min, by immersion with sonication, and then air dried at room temperature. The composite solder paste samples weighed 0.3 g, as measured by an electronic balance. Wettability tests were conducted in argon flow at 250 °C, with a dwell time of 2 min in a tube furnace, and then the samples were cooled in the air. Wetting angles were measured from the cross middle sections in the solidified spreading test specimens, from optical microscope images. The results were compared with monolithic Sn–Ag–Cu solder (see Fig. 2).

2.5 Melting point test

Melting temperatures of the composite solder pastes were investigated by differential scanning calorimetry (DSC Perkin-Elmer Model-7). The DSC samples were pooled from random slices of the solder paste, and the total weight of the sample was less than 10 mg. A sample was placed and sealed in an Al pan which was heated from 30 to 300 °C at a rate of 10 °C/min, under nitrogen atmosphere.

2.6 Microstructural characterization

For microstructural investigation, the composite solder specimens after the wettability test were sectioned for
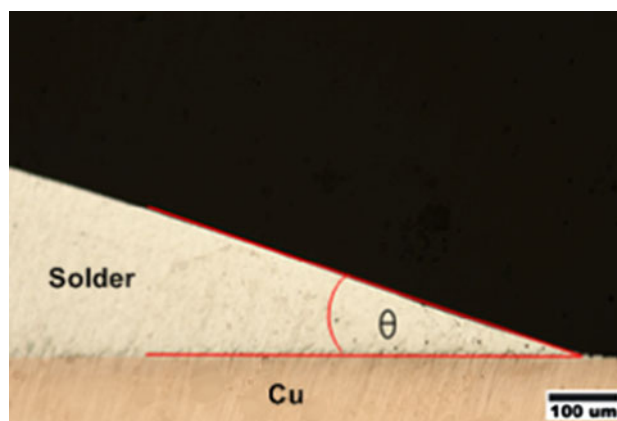
Fig. 2 Contact angle (θ) between composite solder and Cu-substrate: a microscope image of the polished cross-section, of a solidified drop of molten solder

observations. The specimens were cool mounted in epoxy, and then polished to 0.05 μm by alumina (Al$_3$O$_2$) powder finish following standard metallographic techniques, and examined by a SEM Model JSM-5800LV, JEOL. An elemental analysis of the phases was carried out using the energy dispersive X-ray spectroscopy (EDS) function of the SEM.

2.7 Tensile shear test

Tensile shear tests were conducted for investigating effects of reinforcement on mechanical strength of the solder joints. The dimensions of the copper substrate for tensile shear test are 25.4 mm × 80 mm × 3.1 mm. The joint geometry for the test is shown in Fig. 3. Before an experiment, the copper substrate was polished using 400 grit sand paper, then cleaned with distilled water and dried at room temperature. Then, the composite solder paste was enclosed between two such copper substrates. Soldering was performed in an aluminum mold on a hot plate, and solder joints were heated to 250 °C with a dwell time of 2 min. Next, the aluminum mold was removed from the hot plate, placed on a steel plate and cooled in the air. The mechanical properties of the joint specimens were investigating using Hounsfield model H100KS universal testing machine, at a crosshead speed of 1 mm/min, at room temperature. Finally, the specimens were photographed and the fracture surfaces were examined by using SEM Model JSM-5800LV, JEOL.

3 Results and discussion

3.1 Solder wettability test

There are reliable methods to estimate solderability; one of these is the spread test which is a good simulation of the reflow soldering process. In the spread test, the ability of the molten solder to spread over the substrate is used to characterize wetting behavior, usually quantified by the contact angle. The effect of coated nanotube loading on wettability is shown graphically in Fig. 4 and numerically in Table 3. With the addition of 0.01 wt% of Ag-coated SWCNTs, the contact angle decreased by 45.5 %, and an optimum contact angle of 13.8° ± 0.9° was achieved. This could be attributed to the lower surface-interfacial energy when the Ag-coated SWCNTs reinforcement was used [30]. However, when a higher addition of the coated nanotubes up to 0.1 wt% the contact angle increased. This could be due to the presence of more Ag-coated SWCNTs obstruct the melt flow by increasing melt viscosity [30]. Han et al. [30] reported that the addition of Ni-coated carbon nanotubes into 95.8Sn–3.5Ag–0.7Cu solder in the amount of 0.05–0.1 wt% effectively reduced the contact angle, while over addition of the Ni-Coated (0.3 wt%) degraded the effect of wetting. Yu et al. [34] also found that the addition of 0.1 wt% of rare earth elements (RE) improved the wettability of Sn–3.5Ag–0.7Cu solder alloy. Furthermore, similar results on the influence of RE addition on the wetting properties have been reported by Wang et al. [35] for the Sn-Ag-RE composite solder. With the addition of 0.25–0.5 wt% of (La, Ce) RE into Sn–3.5Ag solder alloy improved the wetting property. Optimal spread area and contact angle were achieved with the addition of 0.5 wt% RE, while further addition of RE up to 1.0 wt% degraded the wettability. Wang et al. [35] pointed out that the segregation of RE elements on phase boundary could be responsible for the reduction of boundary energy and surface tension, and thus resulted in the improvement of wettability. Even though, the oxidation on the surface of RE might increase the surface tension and reduce the influence of wetting.
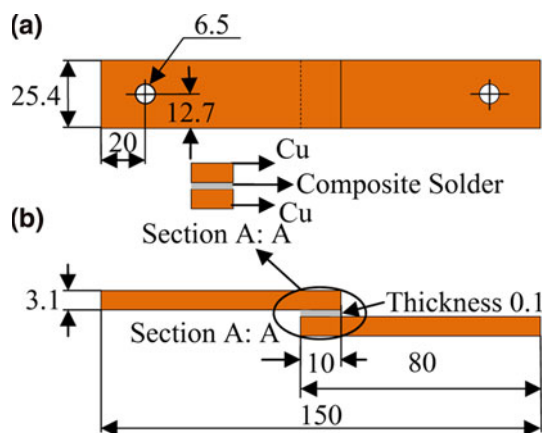
Fig. 3 Schematic diagram of solder joint specimen, **a** *top* view and **b** *side* view. The length unit is millimeters
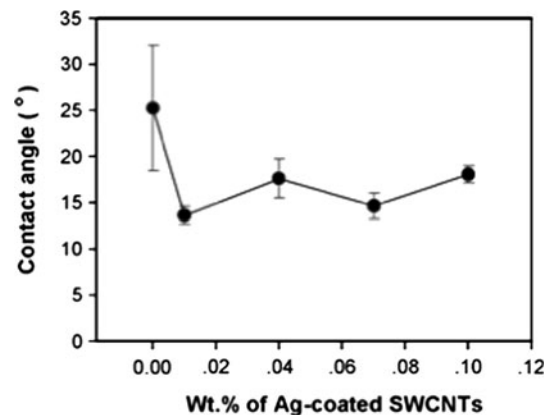
Fig. 4 Relationship between contact angle and weight percentage of Ag-coated SWCNTs in the solder composite

**Table 3** Contact angles of solder composites with different weight percentages of Ag-coated SWCNT

| Material	SWCNTs (wt%)	Contact angle (°)
SAC305	–	25.24 ± 6.80
SAC305-0.01 Ag-coated	0.01	13.76 ± 0.92
SAC305-0.04 Ag-coated	0.04	17.60 ± 2.10
SAC305-0.07 Ag-coated	0.07	14.65 ± 1.37
SAC305-0.10 Ag-coated	0.10	18.03 ± 0.90

3.2 Melting point test

Figure 5 shows DSC curves of the samples reinforced with Ag-coated SWCNTs. Figure 5a shows the baseline of SAC305 without any nanotube loading. Figure 5b shows the DSC scan of SAC305 composite solder reinforced with 0.01 wt% of the Ag-coated SWCNTs. Similarly, Fig. 5c–e show the DSC traces with higher loadings of coated nanotubes. The solidus temperature (T_{onset}) of SAC305 solder was 218.7 °C whereas the peak temperature (T_{peak}) was 221.5 °C. With 0.01 wt% loading of coated nanotubes, T_{onset} and T_{peak} are 218.6 °C and 220.2 °C, respectively. It is evident from Fig. 5 and Table 2 that loading with Ag-coated nanotubes in the range from 0.01 to 0.10 wt% can slightly affect the melting behavior of the composite solders: the peak temperature can be reduced by about 1 °C. Similar results, demonstrating the influence of SWCNT loading on the thermal behavior of composite solder, have been reported

Fig. 5 DSC spectra of SAC305, and SAC305 + Ag-coated SWCNTs composites at different nanotube loadings: **a** SAC305, **b** SAC305 + 0.01 wt%, **c** SAC305 + 0.04 wt%, **d** SAC305 + 0.07 wt% and **e** SAC305 + 0.10 wt%
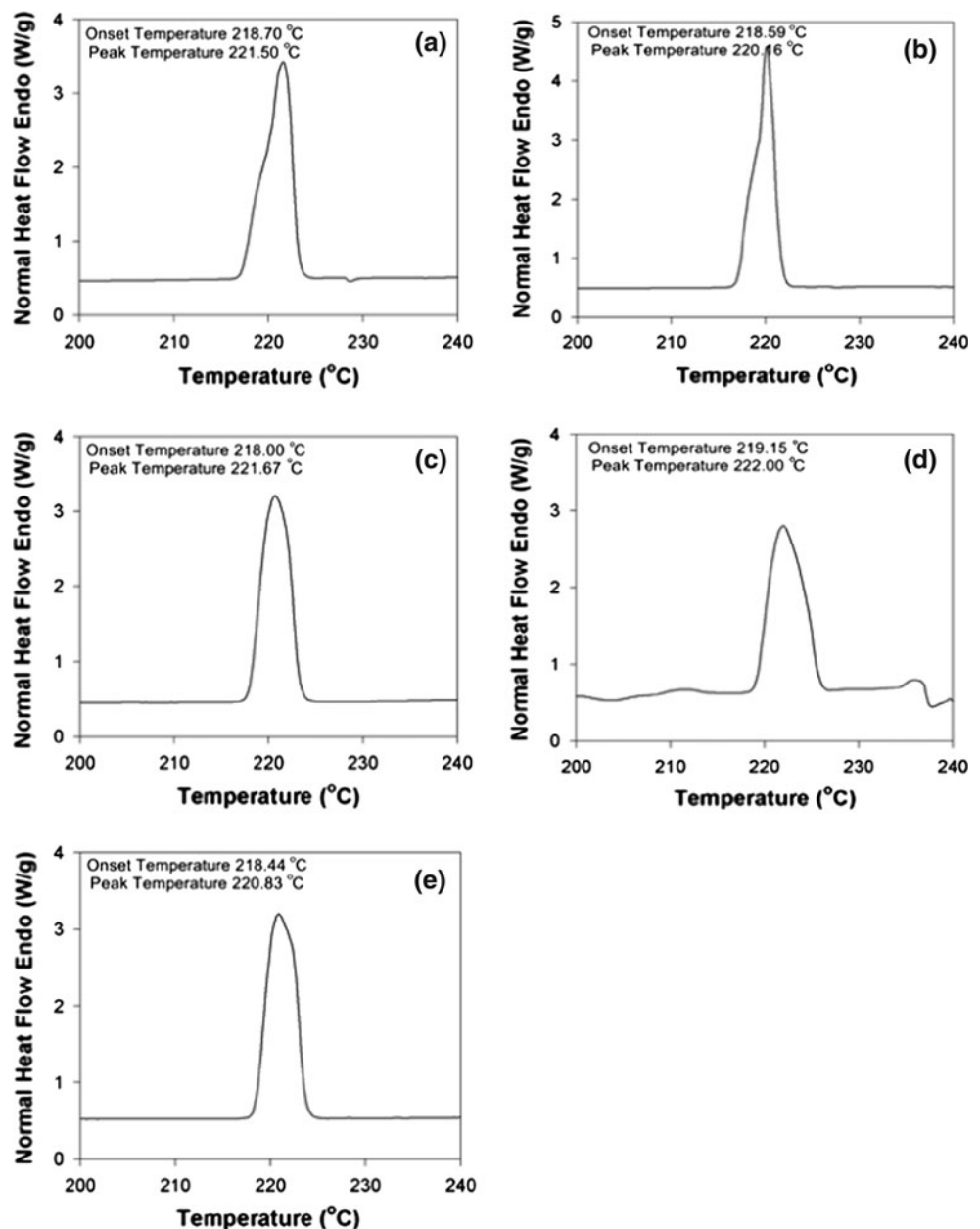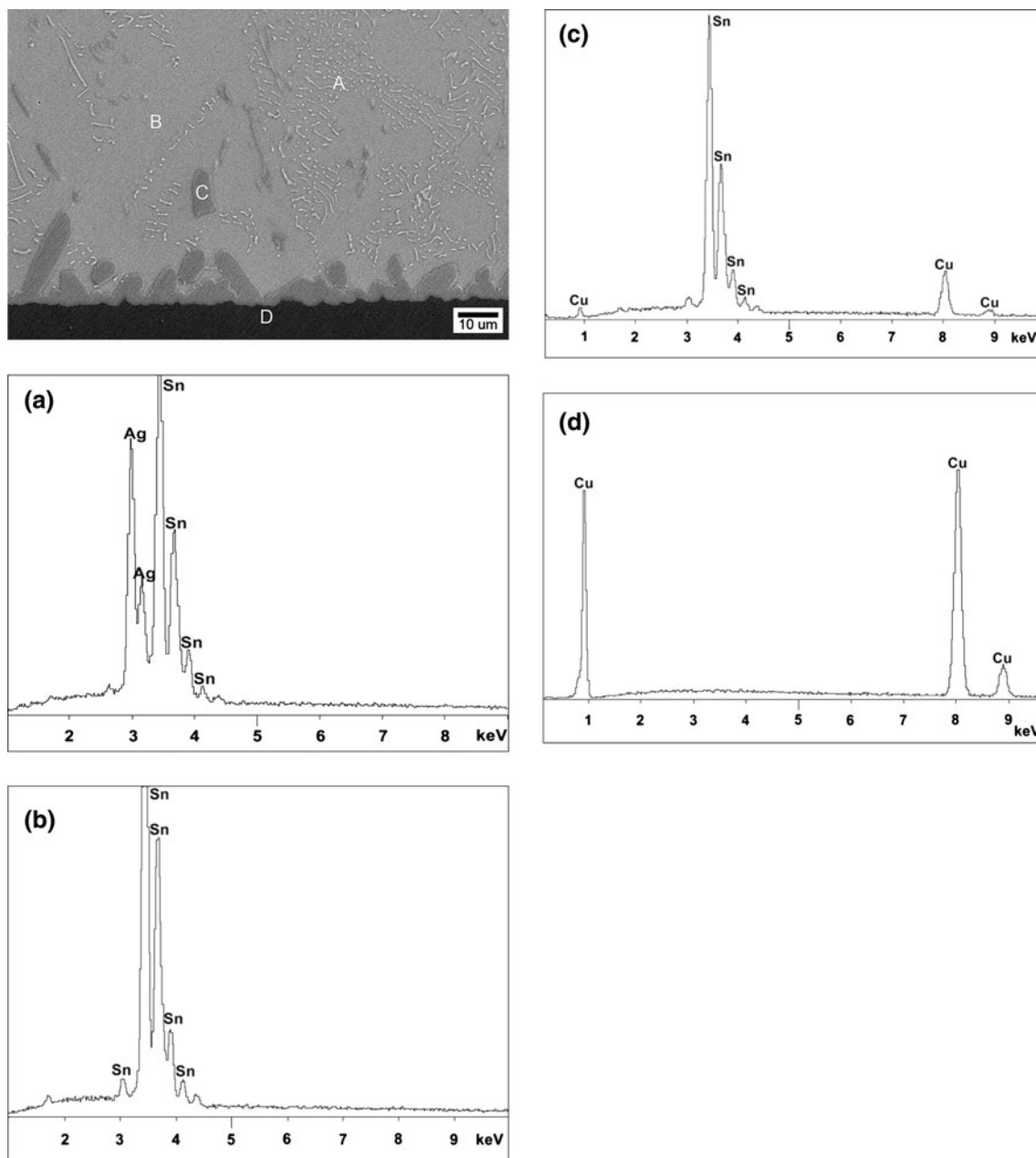
Fig. 6 SEM image of the SAC305 solder on copper, reflowed at 250 °C, and EDS spectra **a–d** corresponding to locations **a–d** marked in the SEM image

by Mohan Kumar et al. [15, 16], for Sn–3.8Ag–0.7Cu–SWCNT lead-free composite solders fabricated by powder metallurgy (PM) approach. The reduction in melting temperature of composite solder was attributed to increased surface instability, due to the increased surface free energy effected by the addition of SWCNTs [14, 16]. On the other hand, Han et al. [30] and Nai et al. [10] reported that there was no significant change in the melting point of addition of MWCNTs into Sn–Ag–Cu solder. This observation does not conflict ours, as the observed effects are marginal in size.

3.3 Microstructural characterization

Figure 6 shows SEM micrographs of the interface between SAC305 solder and Cu substrate reflowed at 250 °C. The microstructure of SAC305 after reflow consists of Sn-rich phases surrounded by small Ag_3Sn phases, and Cu_6Sn_5 is also present in the solder matrix [36, 37]. Most of the Ag_3Sn intermetallic compounds (IMC) phases were formed at the boundaries of Sn-rich phases. Furthermore, the formation of Cu_6Sn_5 is found on the boundary of Sn-rich and

Table 4 Shear strength of solder joints prepared from solder composite mixed with un-coated and Ag-coated SWCNTs at different weight percentages

Material	SWCNTs (wt%)	Max. τ (MPa)	
		Un-coated SWCNTs	Ag-coated SWCNTs
SAC305	–	24.41 ± 1.14	24.41 ± 1.14
SAC305-0.01 SWCNTs	0.01	23.21 ± 1.19	27.12 ± 0.73
SAC305-0.04 SWCNTs	0.04	23.37 ± 1.23	24.35 ± 0.35
SAC305-0.07 SWCNTs	0.07	22.74 ± 2.13	24.83 ± 1.24
SAC305-0.10 SWCNTs	0.10	21.33 ± 1.63	23.47 ± 0.90

**Fig. 7** Shear strength of composite solder joints as a function of wt% SWCNTs

Ag_3Sn regions. These features were qualitatively confirmed by the EDS spectra in Fig. 6a–c. There are many studies on the microstructures of near-eutectic Sn–Ag–Cu composite solders, for example Han et al. [30] investigated the microstructure with addition of Ni-CNT into Sn–Ag–Cu solder. The Ag_3Sn and Cu_6Sn_5 phases were uniformly distributed in the solder matrix. In addition, Kumar et al. [15, 17] and Niranjani et al. [38] have reported on the microstructure of SAC387 alloys also with addition of SWCNTs into SAC387 solder. The IMCs phases were dispersed in the β-Sn matrix, and both Ag_3Sn and Cu_6Sn_5 were equiaxed. It is known that the interfacial IMC layer formed between solder and substrate plays an important role on the reliability of solder joints. Nai et al. [13] reported that the addition of CNTs into Sn–Ag–Cu solder inhibited growth of the IMC. The shear strength of solder joints was dependent on the thickness of IMC layer. The solder joint with thinner IMC layer gained higher shear strength. In the present study, we believe that the addition of Ag-coated SWCNTs into SAC305 solder may have effects on formation of IMC. Therefore, future work is going to look into the dependency of IMC formation and growth on shear strength of solder joints prepared from the Ag-coated SWCNTs composite solder.

3.4 The shear test and fracture surface

The shear test results of solder joints are listed in Table 4 and plotted in Fig. 7, for different Ag-coated SWCNTs loadings in composite solders. The ultimate shear strength increased most with 0.01 wt% of Ag-coated SWCNTs, with an increase of 11 %. For all other composite formulations, the effects on shear properties were insignificant. Similar trends have earlier been reported for the tensile strength of bulk SAC357-MWCNTs composite solders [9–11]. Zhou et al. [39] found that the addition of Bi can improve the shear strength of Sn–Zn–Bi lead-free solder
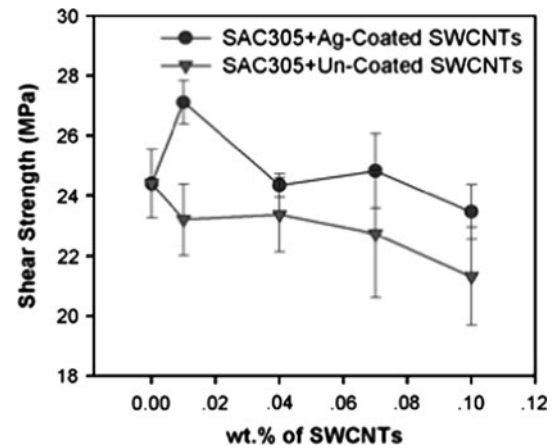
alloy. With the addition of 4 wt% Bi element to the solder matrix, the composite solder joints had higher shear strengths than the monolithic composite solders. Similarly, it was reported that too much reinforcement (such as 10 wt% Bi element) decreased the shear strength. Furthermore, similar results on the influence of MWCNT addition on the shear strength of composite solder have been reported by Nai et al. [12, 13], for Sn–3.5Ag–0.7Cu–MWCNT lead-free composite solders fabricated by powder metallurgy. Improvements in mechanical properties can be attributed to the following mechanisms: (1) generation of geometrically necessary dislocations to accommodate thermal and elastic modulus mismatch between solder matrix and CNTs, (2) load-bearing effects due to presence of CNTs and (3) Orowan strengthening whereby dislocation loops form as dislocations by-pass the nanosize CNTs [12, 13]. Representative fractographs of our specimens are presented in Fig. 8, for SAC305 + 0.01 wt% Ag-coated SWCNTs and SAC305 + 0.10 wt% Ag-coated SWCNTs. The fracture surface analysis of SAC305 + 0.01 wt% Ag-coated SWCNTs revealed the presence of well-dispersed coated nanotube clusters on the surface. The reduction in shear strength for these specimens, with excess nanotube loading, may be due to the increasing presence of CNTs clusters, which are sources of weakness in the specimens [30, 40]. This observation is evident in Fig. 8c, d showing the fractograph of the SAC305 + 0.10 wt% Ag-coated SWCNTs specimen: clusters of entangled carbon nanotubes were observed. This clustering phenomenon prevented effective bonding between the Ag-coated SWCNTs and the composite solder matrix. Consequently, the formed microporosity acts as stress concentration sites or structural defects, allowing initiation of minimal cracks that eventually led to the failure of the composite solder material.
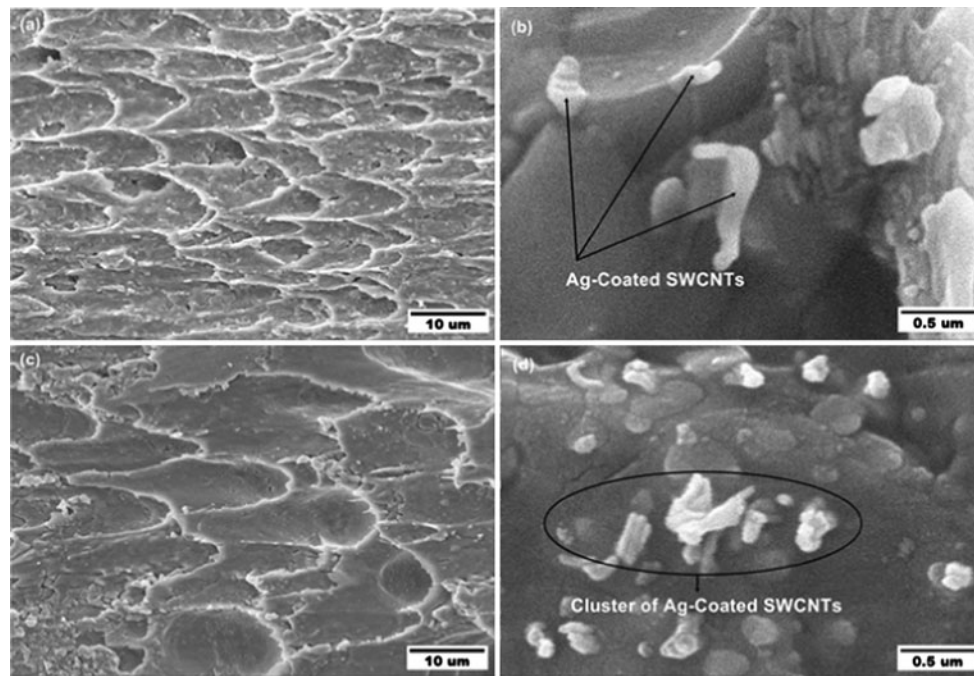
Fig. 8 SEM fractographs showing the fracture surface of composite solder joints, **a, b** SAC305 + 0.01wt% Ag-coated SWCNTs, **c, d** SAC305 + 0.10 wt% Ag-coated SWCNTs

4 Conclusions

The following conclusions could be drawn from the experimental results:

1. The Sn–Ag–Cu composite solder paste reinforced with Ag-coated SWCNTs was successfully synthesized by an ultrasonic mixing technique.
2. The wettability of the composite solder was improved by 45.5 % as loading with 0.01 wt% Ag-coated SWCNTs, and a minimal contact angle of $13.8° \pm 0.9°$ was observed, while over loading of coated nanotubes up to 0.10 wt% reduced the influence of wetting.
3. From the DSC observations, the Ag-coated SWCNTs loading in the range from 0.01 to 0.10 wt% slightly affected the melting behavior of the composite solders: the peak temperature was reduced by about 1 °C.
4. The microstructure results revealed uniformly distributed IMC throughout the solder matrix, and EDS analysis identified the phases as β-Sn, Ag_3Sn and Cu_6Sn_5.
5. A shear strength improvement of 11 % was observed with the addition of only 0.01 wt% Ag-coated SWCNTs in the composite solder—this was the smallest loading in the experimental design, and optimizing the loading for shear strength might give even larger improvements. The Ag-coated SWCNTs had a clustering tendency observed at the higher loadings, that may have reduced the shear strength: the competition between reinforcement and this reduction mechanism is the reason why an optimal loading exists.

References

1. M. Abtew, G. Selvaduray, Mater. Sci. Eng. R **27**, 95 (2000)
2. J.H.L. Pang, B.S. Xiong, IEEE transactions on components and packing technologies. 28, 830 (2005)
3. P.K. Muthur Srinath, P.B. Aswath, J. Mater. Sci. **42**, 7592 (2007)
4. A. Lee, K.N. Subramanian, J. Electron. Mater. **34**, 1399 (2005)
5. F. Guo, J. Mater. Sci. Mater. Electron. **18**, 129 (2007)
6. J. Shen, Y.C. Chan, Microelectron. Reliab. **49**, 223 (2009)
7. S. Iijima, Nature **354**, 56 (1991)
8. S.M.L. Nai, M. Gupta, J. Wei, Int. J. Nanosci. **4**, 423 (2005)
9. S.M.L. Nai, J. Wei, M. Gupta, Thin Solid Films **504**, 401 (2006)
10. S.M.L. Nai, J. Wei, M. Gupta, Mater. Sci. Eng. A **423**, 166 (2006)
11. S.M.L. Nai, J. Wei, M. Gupta, J. Electron. Mater. **35**, 1518 (2006)
12. S.M.L. Nai, J. Wei, M. Gupta, J. Electron. Mater. **37**, 515 (2008)
13. S.M.L. Nai, J. Wei, M. Gupta, J. Alloys. Compd. **473**, 100 (2009)
14. Z.Q. Xue, W.M. Liu, S.M. Hou, J.P. Sun, Z.J. Shi, Z.N. Gu, X.Y. Zhao, Z.X. Zhang, J.L. Wua, L.M. Peng, Q.D. Wu, Mater. Sci. Eng. C **16**, 17 (2001)

15. K.M. Kumar, A.O. Andrew, V. Kripesh, J. Alloys Compd. **450**, 229 (2008)
16. K.M. Kumar, V. Kripesh, A.O. Andrew, J. Alloys Compd. **455**, 148 (2008)
17. K.M. Kumar, V. Kripesh, L. Shen, A.O. Andrew, Thin Solid Films **504**, 371 (2006)
18. Y. Feng, H. Yuan, J. Mater. Sci. **39**, 3241 (2004)
19. H.Y. Song, X.W. Zha, Phys. Lett. A **374**, 1068 (2010)
20. H. Liu, G. Cheng, R. Zheng, Y. Zhao, C. Liang, Diam. Relat. Mater. **15**, 15 (2006)
21. F.Z. Kong, X.B. Zhang, W.Q. Xiong, F. Liu, W.Z. Huang, Y.L. Sun, J.P. Tu, X.W. Chen, Sure. Coat. Technol. **155**, 33 (2002)
22. W.M. Daoush, B.K. Lim, C.B. Mo, D.H. Nam, S.H. Hong, Mater. Sci. Eng. A **513**, 247 (2009)
23. C. Xu, G. Wu, Z. Liu, D. Wu, T.T. Meek, Q. Han, Mater. Res. Bull. **39**, 1499 (2004)
24. W.L. Liu, S.H. Hsieh, W.J. Chen, Appl. Surf. Sci. **253**, 8356 (2007)
25. D.L. Zhao, X. Li, Z.M. Shen, Comps. Sci. Technol. **68**, 2902 (2008)
26. X. Ma, X. Li, N. Lun, S. Wen, Mater. Chem. Phys. **97**, 351 (2006)
27. F. Wang, S. Arai, M. Endo, Carbon **43**, 1716 (2005)
28. X. Chen, J. Xia, J. Peng, W. Li, S. Xie, Compos. Sci. Technol. **60**, 301 (2000)
29. Y.D. Han, H.Y. Jing, S.M.L. Nai, L.Y. Xu, C.M. Tan, J. Wei, Int. J. Nanosci. **9**, 283 (2010)
30. Y.D. Han, S.M.L. Nai, H.Y. Jing, L.Y. Xu, C.M. Tan, J. Wei, J. Mater. Sci. Mater. Electron. **22**, 315 (2011)
31. Y.D. Han, H.Y. Jing, S.M.L. Nai, L.Y. Xu, C.M. Tan, J. Wei, Intermetallics **31**, 72 (2012)
32. B. Zhao, B.L. Yadian, Z.J. Li, P. Liu, Y.F. Zhang, Surf. Eng. **25**, 31 (2009)
33. H.Y. Lu, H. Balkan, K.Y. Simon Ng, J. Mater. Sci. Mater. Electron. **17**, 171 (2006)
34. D.Q. Yu, J. Zhao, L. Wang, J. Alloys. Compd. **376**, 170 (2004)
35. L. Wang, D.Q. Yu, J. Zhao, M.L. Huang, Mater. Lett. **56**, 1039 (2002)
36. S. Kang, D.Y. Shih, N.Y. Donald, W. Henderson, T. Gosselin, A. Sarkhel, N.Y. Charles Goldsmith, K. Puttlitz, W. Choi, JOM **55**, 61 (2003)
37. J.H.L. Pang, L. Xu, X.Q. Shi, W. Zhou, S.L. Ngoh, J. Electron. Mater. **33**, 1219 (2004)
38. V.L. Niranjani, B.S.S. Chandra Rao, V. Singh, S.V. Kamat, Mater. Sci. Eng. A **529**, 257 (2011)
39. J. Zhou, Y. Sun, F. Xue, J. Alloys. Compd. **397**, 260 (2005)
40. A.M.K. Esawi, M.A. El Borady, Compos. Sci. Technol. **68**, 486 (2008)